Virtual Energy Regulator: A Time-Independent Solution for Control of Lower Limb Exoskeletons

Rezvan Nasiri[1,2,*], Mohammad Shushtari[1], Hossein Rouhani[2], *Member*, *IEEE*, and Arash Arami[1,3,**], *Member*, *IEEE*

***Abstract*—In this paper, we introduce a novel control strategy called Virtual Energy Regulator (VER) for lower limb rehabilitation exoskeletons. Unlike the conventional trajectory tracking controllers, VER, which is a time-independent controller, does not control the exoskeleton joints over a reference trajectory. Instead, it imposes a constraint in the state-space and consequently creates a limit cycle behavior for each joint. The time-independent property of VER can resolve the human-exoskeleton coordination problem. The analytical perspectives of VER are studied in detail where we present the limit cycle existence conditions, considerations for the definition of the desired limit cycles, convergence proof, and limit-cycles synchronization. Finally, to support the presented mathematics, we apply the designed VER on Indego exoskeleton (without human) to perform a limit-cycle behavior similar to walking. The experimental and simulation results show that VER generates stable and synchronized limit-cycles at the joints. Our experimental and simulation results support our analytical findings and demonstrate the efficacy of VER for lower limb exoskeletons.**

***Index Terms*—Exoskeleton Control, Rehabilitation, Time-Independent Controller, Limit Cycle, Energy Controller.**

I. Introduction

Every year, between 250,000 and 500,000 people suffer from Spinal Cord Injury (SCI) around the world [1]. A high portion of them have incomplete Spinal Cord Injuries (iSCI), and those with ASIA score of C and D are capable of restoring their walking ability [2]. Due to pieces of evidence on the neuroplasticity of neuromuscular system [3], in iSCI individuals, early physical therapy with rehabilitation exoskeletons may lead to a better neuromotor recovery outcome. To maximize the rehabilitation outcome, the rehabilitation and assistance level should be adapted to the needs of each individual user; i.e., Assist-as-Needed (AAN) [4], [5]. Hence, we can enable them to continue the intensive training while remaining engaged.

There are several methods which tried to realize AAN controller for rehabilitation exoskeletons, ranging from force control [6] and trajectory control [7] to pure reflex-based controllers [8], [9]. As conclusion, it is shown that the pure position control strategy is not effective for iSCI rehabilitation since it does not encourage users to actively contribute to the motion [10]. The position controller considers user dynamics as an external disturbance and tries to reject the user contribution. Besides, from the user's perspective, motions should be completely coordinated with the exoskeleton reference trajectory to benefit from a position tracking controller, which is a major restriction for individuals with neuromuscular impairments; human-exoskeleton coordination problem.

To resolve this problem, various modifications were applied to the pure trajectory tracking controllers. In one approach, the reference trajectory is adapted to minimize the interaction-force between exoskeleton and human; see [4], [11], [12]. This method results in a trajectory more compatible with the user's intended motion. However, in cases with SCI, the trajectory of the user is not reliable. Another approach is to make the controller time-independent.

Variable impedance control was used in the control of wearable robots [13-15] and gait training systems such as Lokomat [16]. Such impedance control strategies ensure the closeness of user trajectory to the reference trajectory at high-impedance regions and allow more flexibility to the user at low-impedance part of the gait cycle. However, the impedance control alone cannot guarantee an optimal cyclic motion, it requires robot's dynamics or interaction force sensing which are missing in many exoskeletons, and the ideal variable joint impedance is not fully known for multi-joint systems during walking, despite some recent studies on single joint impedance identification [17], [18].

As another instance, [4], [5] design a path-controller with position and time tunnels over the designed path which provides the user with some voluntary motions and time-shift about the path. However, the controller is not time-independent, it only tolerates some lead/lag from the reference trajectory. In other attempts to design time-independent controllers, researchers present a joint-space AAN controller by the design of a velocity-dependent vector field [19-21].

Natural Dynamics Exploitation (NDE) techniques, proposed in legged locomotion, could also benefit the human-robot interaction in exoskeletons. Adaptive Natural Oscillators (ANO) [22], [23], Central Pattern Generators (CPG) [24], and Dynamic Movement Primitive (DMP) [25] are examples of NDE methods in robotics. NDE methods prescribe cyclic motions compatible with the natural dynamics of the robot and consequently minimize their energy consumption. From a rehabilitation perspective, having a cyclic motion with

Manuscript received: February, 24, 2021; Revised June, 08, 2021; Accepted July, 5, 2021.

This paper was recommended for publication by Editor Pietro Valdastri upon evaluation of the Associate Editor and Reviewers' comments.

This work is supported by NSERC Discovery, and the New Frontiers in Research Fund under Grant NFRFE-2018-01698.

[1] Department of Mechanical and Mechatronics Engineering, University of Waterloo, Waterloo ON, Canada. [2] Department of Mechanical Engineering, University of Alberta, Edmonton, AB, Canada. [3] Toronto Rehabilitation Institute, University Health Network, Toronto, ON, Canada.

[*] Corresponding author: rezvan.nasiri@uwaterloo.ca.

[**]Principal Investigator: arash.arami@uwaterloo.ca.

Digital Object Identifier (DOI): see top of this page.

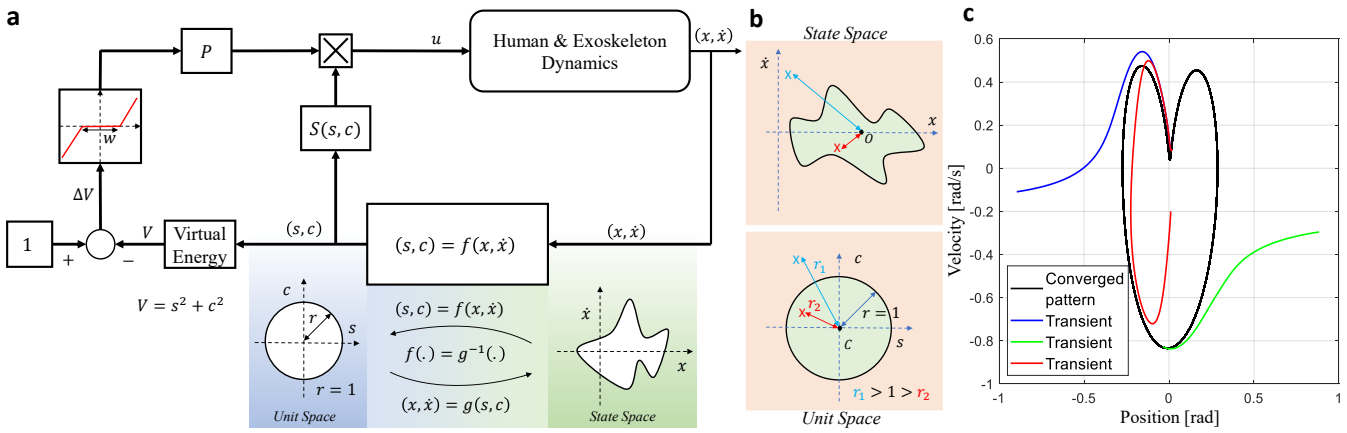

Fig. 1. (a) Control block diagram of "*Virtual Energy Regulator*" for each joint of exoskeleton in which the desired limit-cycle in state-space maps to the unit-circle in the unit-space using $(s, c) = f(x, \dot{x})$ function. Dead-zone block provides a tuning parameter for the user to have voluntary motions about the desired limit-cycle. P is the controller gain which amplifies deviations from the limit-cycle. S is the multiplier which determines the controller gradient. (b) The properties of $(s, c) = f(x, \dot{x})$: (1) it maps O to C, (2) it keeps the distance-inequality after transformation, (3) it maps the points inside, outside, and on the limit-cycle into the inside, outside, and on the unit-circle. (c) The heart-shape limit-cycle generated by VER for a pendulum system.

minimum exoskeleton effort can increase user engagement; this method indirectly leads to an AAN controller.

Recently, a new class of NDE methods is presented which control the mechanical energy of the system instead of imposing a reference trajectory; see [26-28]. Nevertheless, these methods are restricted to some specific types of trajectories computed over mechanical energy eigenmanifold [28]. In this paper, we present a new class of mechanical energy regulators called Virtual Energy Regulator (VER) that projects the desired joint-space limit-cycle into the unit mass-spring dynamics and controls its mechanical energy. In addition, we resolve the problem of independent limit-cycles synchronization which grants a global awareness to the localized limit-cycles at each joint. In conclusion, VER results in stable, time-independent, and synchronized limit-cycles, which grant natural robustness to the controller and contribute to resolving human-exoskeleton miss-coordination.

II. Problem Statement

Fig.1a describes the overall schematic of the VER for each joint of exoskeleton. Unlike the time-based position control that imposes a trajectory as a function of time, VER controls the state-space of each joint over a desired limit-cycle. In this control schematic, $(s, c) = f(x, \dot{x})$ is a bijective function from states-space $(x, \dot{x})$ to unit-space (s, c) which maps the desired limit-cycle to the unit-circle; $s^2 + c^2 = 1$. In the unit-space, the dynamics of each joint is projected into a unit mass-spring; i.e., $m\ddot{s} + ks = \tau$ where $c = \dot{s}, m = k = 1$.

The goal is to regulate the mechanical energy ($V(s, c) = c^2 + s^2$) of the unit mass-spring for each joint on 1. The mechanical energy of a unit mass-spring system is not necessarily equivalent to the mechanical energy of the system, hence, we name $V(s, c)$ as the virtual energy of the system. By regulation of virtual energy on $V = s^2 + c^2 = 1$, (s, c) are constrained to move on a unit-circle. Thanks to the bijective mapping between the spaces, moving over unit-circle in the unit-space yields the desired limit-cycle in the state-space.

The "dead-zone block" is added to neglect minor deviations from the reference limit-cycle in state-space. w provides user with a tuning parameter to have the voluntary motions about the desired limit-cycle. P is a positive gain, which determines the VER power to impose the desired limit cycle based on the impairment level of user; the higher impairment the higher P. Finally, S is a multiplier[1] function which determines the gradient of VER output torque (u). Hence, the control rule for jth joint is $u = PS(s, c)(1 - V(s, c))$, and the vector of control commands is written as $\vec{u} = \bar{P}\bar{S}(\vec{s}, \vec{c})(I - \vec{V}(\vec{s}, \vec{c}))$ where n is the number of exoskeleton's controllable joints[2], $\vec{u} \in \mathbb{R}^n$ is the vector of control commands, $\bar{P} \in \mathbb{R}^{n \times n}$ is a diagonal positive definite matrix, $\bar{S} \in \mathbb{R}^{n \times n}$ is a diagonal function, and $\vec{V} \in \mathbb{R}^n$ is the vector of virtual energy of each joint.

III. Mathematical Analysis

In this section, first, we study the advantage of using VER over a trajectory tracking controller. In the next step, we study the considerations and assumptions regarding the computation of $f(.)$. Moreover, we present the assumptions for the existence of the limit-cycle as well as present the convergence proof towards the desired limit-cycle. Finally, we resolve the problem of synchronization of several limit-cycles in different joints of the exoskeleton.

A. Advantage of VER over a trajectory tracking controller

Fig. 2 describes the fundamental difference between a reference trajectory tracking controller and VER. The first

[1]In our mathematics, since we have $(s, c) = f(x, \dot{x})$, we may refer S and V as functions of either (s, c) or $(x, \dot{x})$.

[2]In the rest of the paper, $\bar{A} \in \mathbb{R}^{n \times n}$ represents a matrix, $\vec{A} \in \mathbb{R}^n$ represents a vector, and $A \in \mathbb{R}$ is a scaler

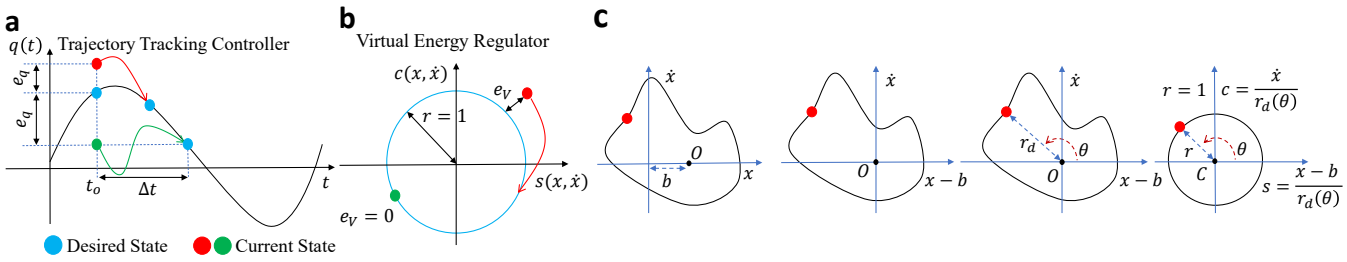

Fig. 2. Difference between trajectory tracking and VER. In trajectory tracking, any violation from the desired trajectory ($q_r(t)$) leads to a controller restriction command which is a function of error and its derivative; $e_q = q_r(t) - q$ and $\dot{e}_q = \dot{q}_r(t) - \dot{q}$. Green and red points show two different initial states (in (a) and (b)), red does not belong to the desired trajectory while green point belongs to it but at a different time ($t = t_o + \Delta t$). Blue points in (a) and blue circle in (b) show desired state. (a) shows a typical desired trajectory and effect of a trajectory tracking based controller, the red and green trajectories are transient trajectories until reaching to a desired state. Even for the cases that the current state belong to the desired trajectory (but in future), the tracking controller only decides based on the current state ($t = t_o$). Hence any time lag/lead between the user and exoskeleton motions leads to a controller restriction command. (b) However, VER is time-independent and the user can start the motion from each desired point on the limit-cycle; it is independent to time-shift. VER applies torque only in cases that the state is not on the limit-cycle, for instance the red point; i.e., $V \neq 1 \rightarrow e_V = 1 - V \neq 0$. (c) A systematic approach to transform limit-cycle to the unit-circle in cases that desired radius (r_d) about O is a function of phase (θ).

difference is that VER makes the system to be fully autonomous; the cyclic behavior is generated only by state-feedback and there is no time-dependent parameter in the controller. In other words, VER provides a bifurcation [29] in the dynamical equations of the human-exoskeleton system and creates a limit-cycle. This property grants natural robustness to the VER compared to trajectory tracking controllers.

In a trajectory tracking controller at a specific moment ($t = t_o$), controller tries to regulate the joint state (both position and velocity) on the desired one; see Fig. 2a. This makes even a specific state which may belong to movement limit-cycle at a different time (for instance $t = t_o + \Delta t$) to be considered as a deviation from the reference trajectory, and the controller tries to work against it. Especially, in lower limb exoskeletons, this behavior restricts the performance of the user to be completely consistent with the dictated reference trajectory by the exoskeleton, i.e., human-exoskeleton coordination problem. VER on the other hand enforces only a constraint to the state-space such that at each joint the projection of states into unit-space should be on the unit-circle (see Fig. 2b), and VER only applies the control command for violation of the specified constraint in the state-space. Accordingly, starting on every single point on the unit-circle does not trigger any control action. Hence, the user can start from any preferable state or switch from one state to another on the desired limit-cycle; VER is robust against user's motion time(phase) shift. Consequently, user can easily coordination with VER due to its time-independency; VER can resolve human-exoskeleton coordination problem.

B. Mapping from desired limit-cycle to unit-circle

To realize VER, $f(.)$ function needs to be formed to map the desired limit-cycle into the unit-circle. $f(.)$ exists if and only if the desired limit-cycle is a simple-closed-curve; i.e., a non-self-crossing-closed-curve. In this case, we call $f(.)$ a topological homeomorphism that maps the simple-closed-curve into a unit-circle; i.e., analytically any simple-closed-curve is homeomorphic (i.e., transformable) to the unit-circle. In this setting, the convergence towards the unit-circle is equivalent to convergence towards the desired limit-cycle. To guarantee this state convergence, $f(.)$ should satisfy the following properties:

i $(s, c) = f(x, \dot{x})$ is a continues function.
ii $(s, c) = f(x, \dot{x})$ is a sufficiently smooth function.
iii $(s, c) = f(x, \dot{x})$ is a bijective function.
iv $(s, c) = f(x, \dot{x})$ is a monotonically increasing function.
v $(s, c) = f(x, \dot{x})$ satisfies the *Jordan Curve Theorem*. Hence, any point inside, outside, and on the limit-cycle are being mapped inside, outside, and on the unit-circle, respectively; see Fig. 1b.
vi $(s, c) = f(x, \dot{x})$ maps a point inside the limit-cycle ('O') to the center of unit-circle ('C'); see Fig. 1b.
vii $(s, c) = f(x, \dot{x})$ keeps the metric property; i.e., the distance-inequality w.r.t. O for each two points in the state-space should be the same as distance-inequality w.r.t. C for the projection of those points in the unit-space; see Fig. 1b.
viii $(s, c) = f(x, \dot{x})$ makes $V = s^2 + c^2$ to be a radially unbounded function of $(x, \dot{x})$.

Presentation of a general method to extract $f(.)$ for any given limit-cycle is still a challenge. Nevertheless, Fig. 2c presents a method to compute $f(.)$ in four steps. This method restricts to the cases that radius (r) of the desired limit-cycle w.r.t. O is a function of its phase (θ); i.e., $r = h(\theta)$. This mapping satisfies all of the mentioned properties. (i) Determine $O = (b, 0)$ point inside the limit-cycle. (ii) Shift O to $(0, 0)$; $(x - b, \dot{x})$. (iii) Compute the phase for each point on the limit-cycle as $\theta = \tan^{-1}(\dot{x}/x)$. (iv) Use a nonlinear mapping to compute the radius as a function of the phase; $r_d = h(\theta)$. The following equations formulate the proposed method.

$$\begin{aligned} &\theta = \tan^{-1}(\dot{x}/x)\ ,\ r_d = h(\theta)\ ,\ r = \sqrt{(x-b)^2 + \dot{x}^2} \\ &s = r/r_d \sin(\theta)\ ,\ c = r/r_d \cos(\theta) \\ &x = r\cos(\theta) + b\ ,\ \dot{x} = r\sin(\theta) \end{aligned} \tag{1}$$

Consider Fig. 1c as a simulation example for the realization of VER to create a heart-shape limit-cycle for a single joint pendulum system. In this example, $f(.)$ is computed using the proposed method in Eq. 1 where $h(.)$ is estimated using a neural network. In addition, Fig. 1c illustrates the convergence behavior towards the stable heart-shape limit-cycle from different initial states.

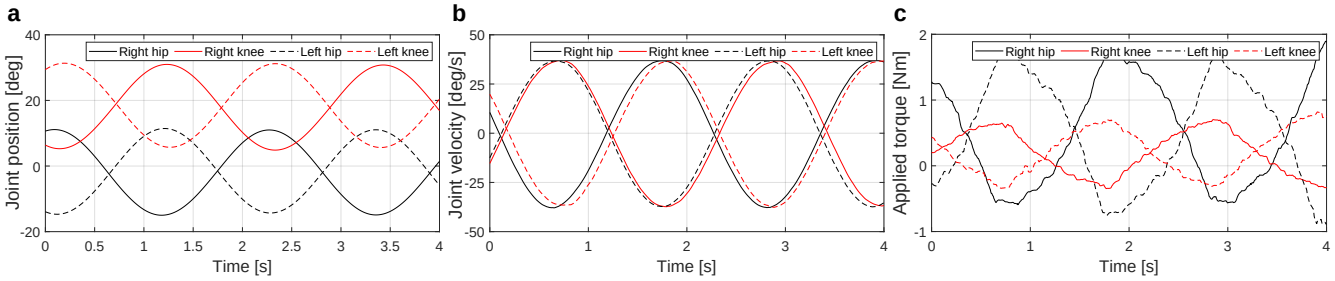

Fig. 3. The experimental results for implementation of VER on Indego exoskeleton at steady-state condition; i.e., after convergence to the limit-cycle. All of the trajectories are smoothed with a window of 200 samples; sampling rate is $200Hz$. In this experiment, limit-cycle parameters are $A = 20deg, \omega = 3rad/s$, and controller parameters are $P_h = 100, P_k = 50, K = 10$. (a,b) are the joint positions and velocities of Indego exoskeleton in the steady-state condition; the joint position is periodic and sinusoidal as it is designed by the desired limit-cycle. (c) describes the torque applied by VER at each joint.

C. Existence of the limit-cycle

Consider the dynamical equations of the human body augmented with an exoskeleton as:

$$\bar{M}(\vec{x})\ddot{\vec{x}} + \vec{C}(\vec{x}, \dot{\vec{x}}) + \vec{G}(\vec{x}) = \vec{u} \tag{2}$$

where $\bar{M} \in \mathbb{R}^{n\times n}$ is a positive definite mass(inertia) matrix[3], $\vec{C} \in \mathbb{R}^n$ is vector of centrifugal coriolis force, and $\vec{G} \in \mathbb{R}^n$ is the vector of gravitational forces. $\vec{x}, \dot{\vec{x}}, \ddot{\vec{x}} \in \mathbb{R}^n$ are position, velocity, and acceleration vectors. $\vec{u}$ is the vector of controller applied torque computed by VER. Based on Poincare-Bendixson criterion [29, pp.61], the necessary condition for the existence of a limit-cycle is that the system should have maximumly one equilibrium point in the limit-cycle domain-of-attraction. To satisfy this condition, the gravity force should not be zero ($\vec{G}(\vec{x}) \neq 0$), which is already satisfied for walking tasks.

D. Limit-cycle convergence Proof

To prove the convergence towards the desired limit-cycle at each joint, consider the vector of virtual energies ($\vec{V}$) as the vector of Lyapanov functions. Accordingly, time derivative of this Lypapanov vector function, is $\dot{\vec{V}} = (\partial\vec{V}/\partial\dot{\vec{x}})\ddot{\vec{x}} + (\partial\vec{V}/\partial\vec{x})\dot{\vec{x}}$. By replacing $\ddot{\vec{x}}$ from Eq.2, we have:

$$\dot{\vec{V}} = \frac{\partial\vec{V}}{\partial\dot{\vec{x}}}\bar{M}^{-1}\bar{S}\bar{P}(I - \vec{V}) - \frac{\partial\vec{V}}{\partial\dot{\vec{x}}}\bar{M}^{-1}(\vec{C} + \vec{G}) + \frac{\partial\vec{V}}{\partial\vec{x}}\dot{\vec{x}}. \tag{3}$$

The elements of $\bar{P}$ are selected sufficiently large such that for each row of Eq. 3 the other terms are negligible compared to the first term ($(\partial\vec{V}/\partial\dot{\vec{x}})\bar{M}^{-1}\bar{S}(I - \vec{V})$). Hence, the approximated dynamics can be written as follows.

$$\dot{\vec{V}} \approxeq \frac{\partial\vec{V}}{\partial\dot{\vec{x}}}\bar{M}^{-1}\bar{S}\bar{P}(I - \vec{V}) \tag{4}$$

$\bar{S}$ should be selected in such a way that $(\partial\vec{V}/\partial\dot{\vec{x}})\bar{M}^{-1}\bar{S}$ is a positive definite matrix. Hence, in Eq.4, for each joint, states within the limit-cycle ($V < 1$) we have $\dot{V} > 0$, and for the states outside the limit-cycle ($V > 1$) we have $\dot{V} < 0$; i.e., the gradient of limit-cycle is convergent towards $V \equiv 1$. Hence, based on *Poincare-Bendixson Criterion* [29, pp.61], VER creates a stable limit-cycle behavior for each joint. The convergence proof is presented without any knowledge about the dynamical equations. In sum, the only considered conditions to have a stable limit-cycle are: (i) gravity vector should not be zero ($\vec{G}(\vec{x}) \neq 0$), (ii) sufficiently large $\bar{P}$, and (iii) selecting $\bar{S}$ such that $(\partial\vec{V}/\partial\dot{\vec{x}})\bar{M}^{-1}\bar{S}$ is a positive definite matrix.

This convergence proof ensures that using VER leads to a stable limit-cycle, however, the generated limit-cycle may not be exactly equivalent to the desired one. To obtain convergence to the desired limit cycle, the presented approximation should be exactly equivalent to the right side of Eq.4. This can be maintained by increasing the $\bar{P}$, however, in complex dynamical systems, increasing $\bar{P}$ can lead to inner instability of the controller or chattering behavior in the actuators. The converged limit-cycle is a combination of natural dynamics of the human-exoskeleton system and the dynamics of the desired limit-cycle. In the case that the designed limit-cycle is fully consistent with the natural dynamics of the human-exoskeleton system, the resultant limit-cycle is the same as desired one. Resolving this interesting problem could be considered as one of our future works.

E. Synchronized limit-cycles

After proving the convergence towards the desired limit-cycles at each joint, it is important to note that satisfaction of $\vec{V}(\vec{x}, \dot{\vec{x}}) \equiv 1$ for all of the joints does not necessary maintain a synchronized behavior across them. Hence, additional control term is required to guarantee the synchronized limit-cycles. Thanks to our well-posed mathematics, we can simply control the phase difference between the limit-cycles using the concept of phase difference on unit-circle. In doing so, to have $0, 90, 180, 270$ degrees phase difference between ith and jth joints, we need to satisfy $c_i \equiv c_j, c_i \equiv s_j, c_i \equiv -c_j, c_i \equiv -s_j$ constrains, respectively. To satisfy these phase difference constraints, additional control terms are added to VER as:

$$\begin{aligned}
&c_i \equiv c_j \rightarrow u_i = K(c_j - c_i)\ ,\ u_j = K(c_i - c_j) \\
&c_i \equiv s_j \rightarrow u_i = K(s_j - c_i)\ ,\ u_j = K(c_i - s_j) \\
&c_i \equiv -c_j \rightarrow u_i = -K(c_j + c_i)\ ,\ u_j = -K(c_i + c_j) \\
&c_i \equiv -s_j \rightarrow u_i = -K(s_j + c_i)\ ,\ u_j = -K(c_i + s_j)
\end{aligned} \tag{5}$$

where K is the phase difference controller gain. Note that the sign of control command is considered so that it provides

[3]In the rest of the paper, we may forbear specifying the argument of the functions; e.g., $\bar{M}(\vec{x})$ may present as $\bar{M}$.

a stabilizer negative feedback for each joint towards the considered phase constraint. Adding the phase constrain controller to VER and synchronizing limit-cycles provides a global awareness between the limit cycles; they will be correlated. In other words, any perturbation/disturbance in one joint lead to a proportional reaction in other joints. In the case that phase difference is designed properly, limit-cycle synchronization can grant mechanical stability in obstacle encounter situations.

IV. Results & Discussion

We analyzed the performance of the proposed controller in experiment with a lower limb exoskeleton and in simulation. In both cases, to have a walking-like cyclic motion, we considered an oval shape limit-cycles ($V(x,\dot{x})$) for hip and knee joints of each leg defined in the following equations[4].

$$\begin{aligned} s_h &= x_h/A,\ c_h = \dot{x}_h/(A\omega) \rightarrow V_h = s_h^2 + c_h^2 = 1 \\ s_k &= (x_k - A)/A,\ c_k = \dot{x}_k/(A\omega) \rightarrow V_k = s_k^2 + c_k^2 = 1 \end{aligned} \tag{6}$$

In this formulation, A and ω determine the range and frequency of motion for each joint. To have a similar to walking behavior, knee and hip joints of each leg should be in phase while two legs should be anti-phase. To reach an anti-phase between two legs, it is sufficient to have 180 degrees phase difference between two hip joints. In conclusion, the control rule for Indego exoskeleton is:

$$\begin{aligned} u_h^R &= S(c_h^R)P_h(1 - V_h^R) + K(c_k^R - c_h^R) - K(c_h^L + c_h^R) \\ u_k^R &= S(c_k^R)P_k(1 - V_k^R) + K(c_h^R - c_k^R) \\ u_h^L &= S(c_h^L)P_h(1 - V_h^L) + K(c_k^L - c_h^L) - K(c_h^R + c_h^L) \\ u_k^L &= S(c_k^L)P_k(1 - V_k^L) + K(c_h^L - c_k^L) \end{aligned} \tag{7}$$

where $S(.)$ here is simply a sign function of c at each joint. To have the synchronized oval-shape limit-cycles, the designed control vector should satisfy four virtual energy constraints (i.e., $e_V \equiv 0$ in four joints) and three phase difference constraints (i.e., $c_k^R - c_h^R \equiv 0, c_k^L - c_h^L \equiv 0, c_h^L + c_h^R \equiv 0$).

Experiment: We implemented VER on an Indego Explorer exoskeleton (Parker Hannifin, USA) [30], without a human user wearing it. We fixed the upper part of the exoskeleton and performed a simplified walking in the air task. The exoskeleton has passive ankle joints and motorized hip and knee joints; see Fig. 4a. It has two different control modes; position and torque control modes where the torque control mode is utilized in this experiment.

The experimental results for implementation of VER on the Indego exoskeleton are presented in Fig. 3; please also check the attached video file. Based on Fig. 3, the proposed controller creates a cyclic behavior (i.e., limit-cycle) in all of the joints. However, as it is discussed in Section III-D, the converged limit-cycle is not exactly the same as the desired one; it is a scale of the desired limit-cycle. The position and velocity of each joint are reported in Fig. 3a and Fig. 3b. The time behavior of the exoskeleton indicates a periodic and coordinated behavior between the joints. As is can be seen, the knee and hip joints at each leg are in phase, and the position of the right and left leg are anti-phase. The exoskeleton applied torque at each joint is presented in Fig. 3c which has a periodic behavior. Finally, the designed controller reaches to on average 10% violation of the limit-cycle constraints and on average less than 4.5% violation from the phase constraints.

[4]In our notations, h and k subscripts refer to hip and knee joints. And, R and L superscripts refer to right and left legs.

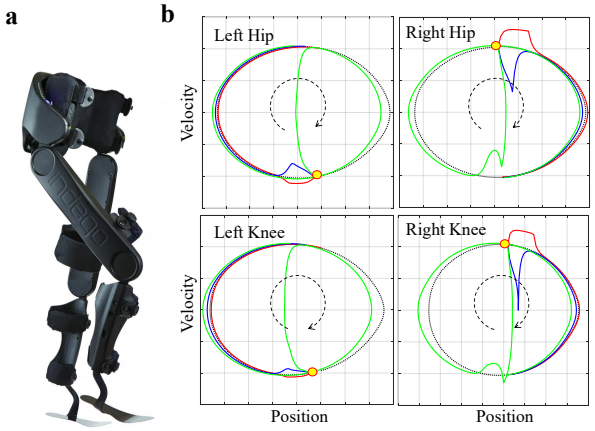

Fig. 4. (a) Indego exoskeleton for lower limb rehabilitation. (b) The robustness study of VER. The disturbance force is applied to the shank of right leg in the sagittal plane; i.e., disturbance force in (x, y) directions are $F_x = F_y = f_d$ where f_d is either $f_d = 0$ (black dashed; steady limit-cycle), $f_d = 45N$ (red solid; disturbed limit-cycle), $f_d = -45N$ (blue solid; disturbed limit-cycle), or $f_d = -60N$ (green solid; disturbed limit-cycle). The yellow point indicates the disturbance instance; comparing this point between the joints show that knee and hip joints in each leg are in phase while two legs are anti-phase. As it can be seen, the disturbance torque applied at the shank of right leg leads to variation in all limit-cycles which shows the performance of synchronization. Interestingly, $f_d = -60N$ leads to a phase shift in the limit-cycle of all joints.

Simulation: A simplified model of Indego is simulated in MATLAB SimMechanics by two independent 2-DOF manipulators; the dynamical parameters of model (mass and length of links) are the same as Indego exoskeleton. The robustness of VER against external disturbances is studied using this model. Moreover, we investigate time-independent nature of VER by a comparative simulation.

The simulation results for the robustness of VER in face of external disturbances are illustrated in Fig. 4b where an external disturbance is applied to the right leg shank. Interestingly, for the small disturbances ($f_d = \pm 45N$), the limit-cycle returns to a state near to undisturbed one while large disturbances ($f_d = -60$) make a significant phase shift in all of the joints. These phase shifts are the result of having synchronized limit-cycles with phase difference constraints. Hence, any phase shift in one of limit-cycles imposes a proportional phase shift to the other ones; see Section III-E. In the case of non-synchronized limit-cycles, this external disturbance only affects the right knee and hip joints while the left leg is moving over its own limit-cycles; this behavior leads to mechanical instability during walking which is the case in trajectory tracking controllers. Nevertheless, having a synchronized limit-cycle provides a global phase awareness between legs, hence, the left leg is also forced to compensate for the phase difference created between two legs due to the

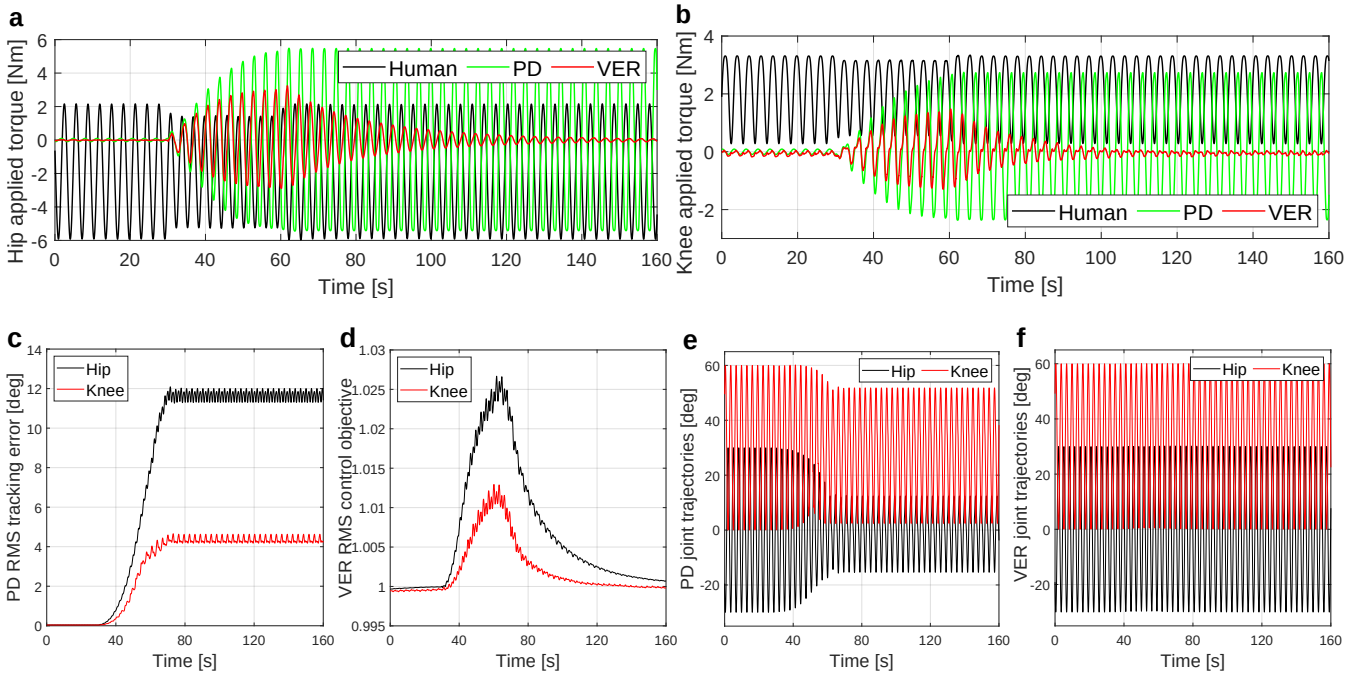

Fig. 5. The comparison between the performance of a trajectory tracking controller (a PD with optimized gains) and VER in presence of human external torque. a) hip torques; b) knee torques; c) PD RMS tracking error; d) VER RMS distance to unit-circle; joint angles using e) PD; and f) VER. During $t \in [0\ 30]s$, the reference trajectory of PD controller and human torque are coordinated, and the performance of both controller are similar. For $t \in [30\ 70]s$ the human torque experiences an additional phase (linearly added) until reaching to $+180deg$, PD controller applies large control commands and fights against human as it cannot minimize the tracking error, and reduces the range of motion. In contrast, VER adapts to the human torque, while satisfying its control objective ($V \equiv 1$), and maintains the range of motion.

external disturbance.

Fig.5 shows the simulation results of controllers interaction with a user. It demonstrates the performance of VER against a trajectory tracking (for comparison we chose a PD) controller for performing the same periodic task; defined as sinusoidal trajectories for PD controller and limit-cycles for VER in Eq.7. In this simulation, human is modeled as a feedforward torque based on his/her intended trajectory. The exoskeleton has an smooth saturation ($\tan^{-1}$ function) on the torque applied at each joint. The saturation boundaries are sufficient to perform the task only by the exoskeleton; $\pm 6Nm$ for hip and $\pm 3Nm$ for knee. The human torque profile can almost fully compensate the required torque for performing the desired motion, hence, an ideal controller should maximally benefit from the human contribution and apply a minimum portion of torque. At first 30 seconds, human torque is coordinated with the reference trajectory (no phase difference) provided to the PD controller, and both controllers maximally benefited from human contribution and apply the minimum torque; see Fig. 5a and Fig. 5b. From $t = 30s$ to $t = 70s$ the phase of human intended trajectory linearly shifts to reach $+180deg$ compared to the PD controller reference trajectory, and consequently the human applied torque linearly shifts up to $+180deg$; the results are the same for lead/lag case. This miss-coordination leads to PD controller torque increment against human contribution; e.g., for $t > 70s$, the human and PD controller torques have opposite signs at the hip joint. In addition, it dramatically increases the PD controller applied torque, and due to the exoskeleton torque saturation, the PD controller cannot perform the task manifested by tracking error increment; see Fig.5c. Furthermore, the conflict between human and PD controller reduces the range of motion by 50%; see hip trajectory in Fig. 5e. Nevertheless, thanks to the time-independent feature of VER, it adapts itself with the human phase variation and still benefits from the human contribution. Moreover, the control objectives (the virtual energies at both of joints should be regulated on 1) and the range of motion in VER controller are always satisfied; see Fig. 5d and Fig. 5f. This simple simulation demonstrates the benefit of VER as a time-independent controller versus trajectory tracking controllers.

V. Conclusion & Future Work

In this paper, we presented a novel control approach called Virtual Energy Regulator and applied it in control of an exoskeleton device. Unlike trajectory tracking controllers, VER is time-independent and applies constraint at the state-space of each joint. As a result, VER generates stable desired limit-cycles at the exoskeleton joints and provides a framework for synchronizing the joint movements.

This paper mainly focused on introducing VER and analytically studies its performance in terms of limit-cycle existence conditions, convergence proof, and synchronization between the joints. In addition, advantages of the proposed

controller over a trajectory tracking controller is discussed. VER has the potential to resolve the human-exoskeleton coordination problem, which is one of the most important issues in the existing exoskeleton controllers.

The proposed VER was successfully implemented on an Indego exoskeleton device without human subject. The experimental results verified the formation of a stable limit-cycle at each joint with the synchronized behavior. The robustness of the VER and limit-cycle synchronization against external disturbance is studied using a simulated model of Indego.

It is explained that due to the inconsistency between the dynamics of exoskeleton and the desired limit-cycle at VER, the resultant limit-cycle might not be exactly the same as the desired one. In fact, the resultant limit-cycle is a nonlinear combination of human-exoskeleton natural dynamics and the considered limit-cycle. In the future work, we will investigate how the designed limit-cycle can be completely compatible with natural dynamics of the system.

One of the limitations of this paper is the lack of human experimental results, however, we believe that VER has the potential to boost the lower limb rehabilitation of individuals with incomplete Spinal Cord Injury, who have residual motor capabilities. Hence, as future work, we will study how to design the limit-cycles for VER to achieve a walking gait for rehabilitation purposes.

REFERENCES

[1] W. H. Organization, "Spinal cord injury," *https://www.who.int/news-room/fact-sheets/detail/spinal-cord-injury*, 2013.

[2] I. Schwartz and Z. Meiner, "Robotic-assisted gait training in neurological patients: who may benefit?" *Annals of biomedical engineering*, vol. 43, no. 5, pp. 1260–1269, 2015.

[3] S. R. Zeiler and J. W. Krakauer, "The interaction between training and plasticity in the post-stroke brain," *Current Opinion in Neurology*, vol. 26, no. 6, p. 609, 2013.

[4] J.-f. Zhang, Y.-m. Dong, C.-j. Yang, Y. Geng, Y. Chen, and Y. Yang, "5-link model based gait trajectory adaption control strategies of the gait rehabilitation exoskeleton for post-stroke patients," *Mechatronics*, vol. 20, no. 3, pp. 368–376, 2010.

[5] A. Duschau-Wicke, J. Von Zitzewitz, A. Caprez, L. Lunenburger, and R. Riener, "Path control: a method for patient-cooperative robot-aided gait rehabilitation," *IEEE Transactions on Neural Systems and Rehabilitation Engineering*, vol. 18, no. 1, pp. 38–48, 2009.

[6] S. K. Banala, S. K. Agrawal, and J. P. Scholz, "Active leg exoskeleton (alex) for gait rehabilitation of motor-impaired patients," in *2007 IEEE 10th International Conference on Rehabilitation Robotics*. IEEE, 2007, pp. 401–407.

[7] J. L. Emken, S. J. Harkema, J. A. Beres-Jones, C. K. Ferreira, and D. J. Reinkensmeyer, "Feasibility of manual teach-and-replay and continuous impedance shaping for robotic locomotor training following spinal cord injury," *IEEE Transactions on Biomedical Engineering*, vol. 55, no. 1, pp. 322–334, 2007.

[8] A. R. Wu, F. Dzeladini, T. J. Brug, F. Tamburella, N. L. Tagliamonte, E. H. Van Asseldonk, H. Van Der Kooij, and A. J. Ijspeert, "An adaptive neuromuscular controller for assistive lower-limb exoskeletons: A preliminary study on subjects with spinal cord injury," *Frontiers in neurorobotics*, vol. 11, p. 30, 2017.

[9] F. Dzeladini, A. R. Wu, D. Renjewski, A. Arami, E. Burdet, E. van Asseldonk, H. van der Kooij, and A. J. Ijspeert, "Effects of a neuromuscular controller on a powered ankle exoskeleton during human walking," in *2016 6th IEEE International Conference on Biomedical Robotics and Biomechatronics (BioRob)*. Ieee, 2016, pp. 617–622.

[10] J. F. Israel, D. D. Campbell, J. H. Kahn, and T. G. Hornby, "Metabolic costs and muscle activity patterns during robotic-and therapist-assisted treadmill walking in individuals with incomplete spinal cord injury," *Physical therapy*, vol. 86, no. 11, pp. 1466–1478, 2006.

[11] E. T. Wolbrecht, V. Chan, D. J. Reinkensmeyer, and J. E. Bobrow, "Optimizing compliant, model-based robotic assistance to promote neurorehabilitation," *IEEE Transactions on Neural Systems and Rehabilitation Engineering*, vol. 16, no. 3, pp. 286–297, 2008.

[12] G. Rosati, J. E. Bobrow, and D. J. Reinkensmeyer, "Compliant control of post-stroke rehabilitation robots: using movement-specific models to improve controller performance," in *ASME International Mechanical Engineering Congress and Exposition*, vol. 48630, 2008, pp. 167–174.

[13] J. A. Blaya and H. Herr, "Adaptive control of a variable-impedance ankle-foot orthosis to assist drop-foot gait," *IEEE Transactions on neural systems and rehabilitation engineering*, vol. 12, no. 1, pp. 24–31, 2004.

[14] R. Jimenez-Fabian and O. Verlinden, "Review of control algorithms for robotic ankle systems in lower-limb orthoses, prostheses, and exoskeletons," *Medical engineering & physics*, vol. 34, no. 4, pp. 397–408, 2012.

[15] M. A. Price and F. C. Sup IV, "A handheld haptic robot for large-format touchscreens," *IEEE/ASME Transactions on Mechatronics*, vol. 23, no. 5, pp. 2347–2357, 2018.

[16] R. Riener, L. Lunenburger, S. Jezernik, M. Anderschitz, G. Colombo, and V. Dietz, "Patient-cooperative strategies for robot-aided treadmill training: first experimental results," *IEEE transactions on neural systems and rehabilitation engineering*, vol. 13, no. 3, pp. 380–394, 2005.

[17] H. Lee, E. J. Rouse, and H. I. Krebs, "Summary of human ankle mechanical impedance during walking," *IEEE journal of translational engineering in health and medicine*, vol. 4, pp. 1–7, 2016.

[18] A. Arami, E. van Asseldonk, H. van der Kooij, and E. Burdet, "A clustering-based approach to identify joint impedance during walking," *IEEE Transactions on Neural Systems and Rehabilitation Engineering*, vol. 28, no. 8, pp. 1808–1816, 2020.

[19] H. J. Asl, T. Narikiyo, and M. Kawanishi, "Neural network velocity field control of robotic exoskeletons with bounded input," in *2017 IEEE International Conference on Advanced Intelligent Mechatronics (AIM)*. IEEE, 2017, pp. 1363–1368.

[20] ——, "An assist-as-needed velocity field control scheme for rehabilitation robots," in *2018 IEEE/RSJ International Conference on Intelligent Robots and Systems (IROS)*. IEEE, 2018, pp. 3322–3327.

[21] A. Martinez, B. Lawson, C. Durrough, and M. Goldfarb, "A velocity-field-based controller for assisting leg movement during walking with a bilateral hip and knee lower limb exoskeleton," *IEEE Transactions on Robotics*, vol. 35, no. 2, pp. 307–316, 2018.

[22] R. Nasiri, M. Khoramshahi, and M. N. Ahmadabadi, "Design of a nonlinear adaptive natural oscillator: Towards natural dynamics exploitation in cyclic tasks," in *2016 IEEE/RSJ International Conference on Intelligent Robots and Systems (IROS)*. IEEE, 2016, pp. 3653–3658.

[23] M. Khoramshahi, R. Nasiri, M. Shushtari, A. J. Ijspeert, and M. N. Ahmadabadi, "Adaptive natural oscillator to exploit natural dynamics for energy efficiency," *Robotics and Autonomous Systems*, vol. 97, pp. 51–60, 2017.

[24] A. J. Ijspeert, "Central pattern generators for locomotion control in animals and robots: a review," *Neural networks*, vol. 21, no. 4, pp. 642–653, 2008.

[25] S. Schaal, "Dynamic movement primitives-a framework for motor control in humans and humanoid robotics," in *Adaptive motion of animals and machines*. Springer, 2006, pp. 261–280.

[26] G. Garofalo and C. Ott, "Energy based limit cycle control of elastically actuated robots," *IEEE Transactions on Automatic Control*, vol. 62, no. 5, pp. 2490–2497, 2016.

[27] M. Nekoui, J. Khaghani, R. Nasiri, and M. N. Ahmadabadi, "Natural dynamics exploitation of dynamic soaring: Towards bio-inspired and energy efficient flying locomotion," in *2018 IEEE/RSJ International Conference on Intelligent Robots and Systems (IROS)*. IEEE, 2018, pp. 8171–8176.

[28] C. Della Santina and A. Albu-Schaeffer, "Exciting efficient oscillations in nonlinear mechanical systems through eigenmanifold stabilization," *IEEE Control Systems Letters*, 2020.

[29] H. K. Khalil, *Nonlinear systems*. Prentice hall Upper Saddle River, 2002.

[30] V. University, "Salisbury d. fda clears parker's indego exoskeleton for clinical, personal use," *https://news.vumc.org/2016/03/10/fda-approves-vanderbilt-designed-indego-exoskeleton-for-clinical-and-personal-use/*, 2016.